Reforming of methane with carbon dioxide over a catalyst consisting of ruthenium metal and cerium oxide supported on mordenite

Keiji Hashimoto *, Seiji Watase and Naoji Toukai
Osaka Municipal Technical Research Institute, Morinomiya Joto-ku Osaka 536-8553, Japan

Received 14 August 2001; accepted 8 February 2002

Reforming of CH_4 with CO_2 proceeds at 400 °C over a catalyst consisting of ruthenium metal and CeO_2 highly dispersed on mordenite. The catalyst, Ru-CeO_2/MZ, is highly active for the reforming of CH_4 under the conditions at which a carbon formation reaction is thermodynamically apt to take place. The reforming selectively forms H_2 and CO. An increase in the weight of the catalyst resulting from carbon deposits was scarcely observed. IR spectra for the catalyst indicate that the reforming proceeds via the formation of the intermediate species such as Ru-CO and Ru-CH_x on the surface of ruthenium. The data of H_2 adsorption support the idea that ruthenium is highly dispersed in Ru-CeO_2/MZ.

KEY WORDS: ceria; mordenite; ruthenium; methane reforming; CO_2.

1. Introduction

Reforming of CH_4 with CO_2 is useful for conversion of CH_4 to H_2 and CO as chemical raw materials and fuel gas of fuel cells. In particular, carbon dioxide causing global warming is effectively available to reduce it. There are many studies on reforming [1–10]. Reforming has been carried out at high temperature, because this thermodynamically gives an equilibrium on the production side, and the carbon deposits causing the deactivation of the catalyst often occur at a lower temperature, though the construction costs of its plant can be reduced by reforming at lower temperature. It is therefore important to develop a highly-active catalyst with poison resistance, able to withstand carbon deposits at low temperature. Cerium oxide possesses unique features, such as stabilization of noble metal dispersion [11–14] and the ability to improve the storage of oxygen [15–18]. It is expected that an increase in the storage of oxygen enhances the oxidation of carbon deposited on the catalyst and so could moderate carbon deposits. We have previously reported [19] that the fine particles of CeO_2 incorporated into zeolite cavities are highly activated, which accelerates the oxidation of alkyl benzenes, and that the catalyst consisting of ruthenium metal and cerium oxides supported on Y-form zeolite represses hydrogen inhibition in NH_3 decomposition [20]. In this paper, we report the preparation of ruthenium and CeO_2 highly dispersed on mordenite, high activity for the CH_4 reforming with CO_2, and adsorption species on the surface of ruthenium.

* To whom correspondence should be addressed.

2. Experimental

2.1. Materials

All chemicals were analytical grade commercial materials and used without further purification. The proton form of mordenite (JRC-Z-20HM) was supplied by the Catalyst Reference Committee of the Japan Catalysis Society. Methane (more than 99.99%) and carbon dioxide gas (more than 99.9%) were dried by passing through a packed bed of a 4 Å molecular sieve.

2.2. Preparation of Ru-CeO_2/MZ catalyst

The catalyst consisting of ruthenium metal and cerium oxides supported on mordenite was prepared by a method similar to that reported earlier [19]. The chemical composition of Ru-CeO_2/MZ was analyzed by inductively coupled plasma (ICP) measurements. The results are summarized in table 1. The contents of SiO_2, Al_2O_3, CeO_2 and Ru were determined to be 87.1, 7.4, 4.5 and 0.29 wt%, respectively.

2.3. Reforming of CH_4 with CO_2

The reforming of CH_4 with CO_2 was carried out in a fixed-bed pulse-flow microreactor made from a 1.5 mm i.d. stainless steel tube and under the conditions at which the carbon formation reactions were thermodynamically apt to be brought about by using $CO_2/CH_4 = 1–0.3$ at 400–450 °C. The catalyst (0.015 g) was sandwiched with quartz wool in the pulse microcatalytic reactor. The catalyst was heated for 2 h at 400 °C under a carrier gas prior to the reaction and then to a fixed reaction

1011-372X/02/0600-0147/0

Table 1
Chemical composition

Composition	Ru/CeO_2-MZ (wt%)
SiO_2	87.1
Al_2O_3	7.4
CeO_2	4.5
Ru	0.29
Na_2O	0.05
Ig. loss	4.9

Note: The weight loss of the catalyst is 4.9 wt% on evacuation at 500 °C for 30 min.

temperature. A pulse of $0.5–1.5 \times 10^{-6}$ mol of CH_4 and CO_2 in a proportion of 1:0.8–0.3 (He balance) was injected into the catalyst bed. The pulse injection of $CH_4 + CO_2$ was repeated several times to check the reproducibility of the reaction. The reaction mixtures were analyzed using GC connected with a pulse microreactor with a helium or nitrogen flow rate of 10 ml min^{-1}; nitrogen carrier gas was used when determining hydrogen. The space velocities were 80 000 h^{-1}. The stainless steel tube and quartz wool (packing material) make no contribution to the reforming.

2.4. Decomposition of CH_4

The decomposition of CH_4 was carried out in a fixed-bed tubular reactor with a constant volume (83 ml). The reactor, made from a 6 mm i.d. glass tube, is equipped with an MKS Baratron 627 transducer pressure gauge to monitor the decomposition and with an electric furnace, and connected to a vacuum line. The catalyst (0.050 g) was placed in the reactor. The sample was pretreated *in vacuo* for 3 h at 400 °C. The sample was exposed at a fixed temperature at a pressure of ~10 kPa of CH_4. The decomposition rate was determined on the basis of an increase in reaction pressure resulting from CH_4 decomposition.

2.5. Weight variation of the catalyst with reaction time

The weight variation with reaction time was recorded using a Rubotherm magnetic suspension balance connected to a vacuum line. The catalyst (0.08 g) was placed on the sample pan in the balance and pretreated at 400 °C for 2 h *in vacuo* prior to the reforming and decomposition. The catalyst was then exposed to 5–10 kPa of a mixture of CO_2 and CH_4 in the proportion $CO_2:CH_4 = 1:1$ at a fixed temperature. The amount of carbon deposit was determined by the increase in weight of the catalyst from the base at the reaction time zero.

2.6. X-ray powder diffraction measurements (XRD)

XRD patterns of the samples were recorded using a Mac-Science 18 spectrometer (Ni-filtered Cu K_α, 40–100 kV, 50–100 mA). The samples were mounted on sample boards and the measurements were immediately carried out.

2.7. FTIR measurements

FTIR spectra were recorded on a Shimadzu 8100 FTIR spectrometer using a conventional IR cell connected to a vacuum line and adsorption apparatus. About 0.010 g of the catalyst was compressed at 7.5 tons cm^{-2} using a pellet die to form a 10 mm diameter circular disk. All samples were pretreated *in vacuo* for 2 h at 450 °C before the FTIR measurements. First, the spectra for the degassed sample were measured as a reference spectrum. The sample was then exposed at 450 °C for a fixed reaction time to CO_2, CH_4 or a mixture of these gases, prior to FTIR measurements. The FTIR measurements in the absence of the sample were carried out 40 times at room temperature to obtain a blank spectrum and then those for the sample were similarly done. The integrated spectrum was obtained and then revised by subtracting the blank spectrum due to gas-phase and/or products condensed on the windows of IR cell.

3. Results and discussion

3.1. Reforming of CH_4 with CO_2

The reforming of CH_4 with CO_2 was studied using a pulse-flow reaction under the conditions at which the carbon formation reactions over the catalyst were rapidly brought about by using $CO_2/CH_4 = 0.8–0.3$ at 400–450 °C (He or N_2 balance). The results are summarized in table 2. The reforming selectively forms H_2 and CO and the ratio of CO to H_2 is nearly equal to 1 in each experiment, whereas no reforming proceeds in the absence of Ru. The amount of one-pulse injection is $0.5–1.5 \times 10^{-6}$ moles of CH_4 and CO_2 in a proportion of 1:0.8–0.3 as starting feed. On the other hand, Ru-CeO_2/MZ (15 mg) packed in the microreactor contains 4.3×10^{-7} mol of ruthenium. The turnover frequency (TOF) values of the catalytic sites were estimated by considering that each ruthenium atom was exposed to the reaction mixture and was able to produce syn-gas. This assumption is based on the amount of hydrogen chemisorption as described below. The TOF is calculated to be 1.7 and 7.0 s^{-1} at 400 and 450 °C, respectively. It is reported that the TOF is 5.1 s^{-1} at 750 °C for Rh/Al_2O_3 [1], 1.2 s^{-1} at 600 °C and 4.0 s^{-1} at 700 °C for Rh/Al_2O_3 [21], 2.1 s^{-1} at 500 °C for Ir/Al_2O_3 [21], 1.8 s^{-1} at 450 °C for Pt/TiO_2 [22], and 3.5 s^{-1} 600 °C for Pt/Al_2O_3 [23]. The TOF value in the reforming increases generally with an increase in reaction temperature. The TOF values of Ru-CeO_2/MZ are high, compared with the highly active noble-metal catalysts

Table 2
Product distribution of CH_4 reforming with CO_2

Reaction temperature (°C)	Pulse [a] (μmol)	CO_2/CH_4	Conversion (%)	$CO + H_2$ (%)	CH_4 (%)	CO_2 (%)
400	0.5	0.7	6.5	14.2	51.0	34.8
400	0.5	0.8	6.6	13.4	47.5	39.1
450	1.4	0.3	9.7	26.5	62.0	11.5
450	1.0	0.7	14.2	28.2	42.7	29.1
450	1.3	0.6	9.9	22.1	50.5	27.4
450	1.1	0.7	12.6	26.2	45.3	28.5

Note: The conversion was determined from CH_4 base. Catalyst: 0.015 g.
[a] The amount of pulsed CH_4. Flow rate of He or N_2: 10 ml min^{-1}; nitrogen carrier gas was used to measure H_2 with GC.

reported in references [1,21–23]. After the exposure of Ru-CeO_2/MZ at 450 °C for 24 h to 8 kPa of a mixture of CO_2 and CH_4 in the proportion $CO_2:CH_4 = 1:1$, the TOF of the catalyst decreased from 7.0 to 3.3 s^{-1} at 450 °C.

3.2. Decomposition of CH_4

The decomposition of CH_4 was studied at 400, 450 and 500 °C: the reaction was carried out in a batch mode, because the reaction rate was so slow that the peak area of a gas chromatography due to the decomposition products was negligible in the pulse-flow reaction. The results are shown in figure 1. The apparent activation energy is calculated to be 5.6 kcal mol^{-1} from Arrhenius plots of the data in figure 1. The value is nearly equal to the activation energy, 6 kcal mol^{-1}, for the CH_4 chemisorption reported in reference [24]. The CH_4 decomposition is thermodynamically very preferable to the refining through the range 400–500 °C. The decomposition rates of CH_4 at 400, 450 and 500 °C are determined to be 1.7×10^{-7}, 2.2×10^{-7} and 2.7×10^{-7} mol g cat^{-1} min^{-1}, respectively (figure 1). The TOF values per ruthenium atom for the CH_4 decomposition are estimated to be less than 0.0002 s^{-1}. These values are very low, compared with those in the reforming. The result hence leads to the conclusion that the presence of CO_2 significantly accelerates the CH_4 decomposition in Ru-CeO_2/Mord.

3.3. Carbon formation

The variation of catalyst weight with an increase in reaction time was studied using a magnetic suspension balance equipped no-diffusion apparatus. The measurements were carried out under the conditions ($CO_2/CH_4 = 1$ at 400–450 °C) at which the carbon formation reactions took place rapidly in the catalyst containing nickel [1]. The results are shown in figure 2. The weight of the catalyst hardly increases with an increase in reaction time, though the weight varies considerably. In the literature [2,21,25], a reaction mechanism which is capable of explaining the carbon formation in the reforming can be represented by the following six elementary steps:

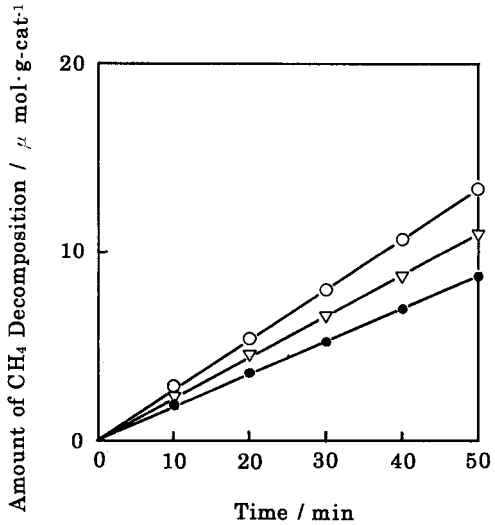

Figure 1. Decomposition of CH_4. ●, 400 °C; △, 450 °C; ○, 500 °C. Reaction volume, 83.5 ml; catalyst, 17.0 mg; initial pressure of CH_4, 8 kPa.

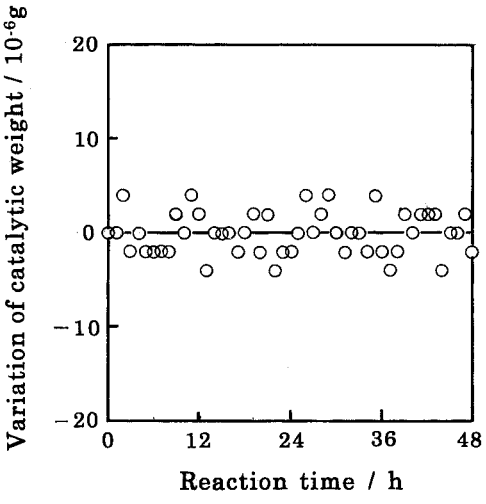

Figure 2. Variation of catalytic weight with reaction time. Catalyst weight, 80 mg; reaction pressure ($CH_4/CO_2 = 1$), 8 kPa; reaction temperature, 450 °C.

$$CH_4(g) + (s) \rightleftharpoons CH_4(s) \quad (1)$$

$$CO_2(g) + (s) \rightleftharpoons CO_2(s) \quad (2)$$

$$CH_4(s) + (4-x)(s) \rightleftharpoons CH_x(s) + (4-x)H(s) \quad (3)$$

$$CH_x(s) + x(s) \rightleftharpoons C(s) + xH(s) \quad (4)$$

$$CO_2(s) + (s) \rightleftharpoons CO(s) + O(s) \quad (5)$$

$$CO(s) + (s) \rightleftharpoons C(s) + O(s) \quad (6)$$

where (g) and (s) represent a gas and adsorption site, respectively. The elementary step (4) is endothermic and carbon formation occurs easily at high temperature at low pressure of CH_4, whereas step (6) is exothermic and proceeds to the right-hand side at low temperature at high pressure of CO_2. The results in figure 2 indicate that carbon deposits resulting from CH_4 decomposition and CO_2 dissociation scarcely occur during the reforming. It is considered that the equilibria in the elementary step (4) and (6) favor the left-hand side through low temperature and low pressure of CO_2, respectively. The depression of the carbon formation is reasonably explained in terms of the favorable equilibriums.

3.4. Characterization of the Ru-CeO_2/MZ catalyst

X-ray diffraction (XRD) patterns were recorded and are shown in figure 3. XRD patterns for Ru-CeO_2/MZ are well in accordance with those for mordenite [26]. The catalyst maintains the structure of mordenite. The XRD peaks, resulting from a cubic crystal structure of CeO_2, appear at $2\theta = 28.6°$, 33.1°, 47.5° and 56.4° [27]. Ruthenium displays XRD at $2\theta = 38.5°$, 42.1°, 44.0° and 58.5° [26]. However, no diffraction pattern due to ruthenium metal and ceria was observed (figure 3). We have already reported [19,20] that the fine particles of CeO_2 incorporated into the zeolite cavities were prepared by a hydrolysis of cerium ions with a moist ammonia gas. The result suggests a high dispersion of ceria in the zeolite. No diffraction patterns due to Ru are explained in terms of high dispersion of Ru and/or its low content.

FTIR spectra were measured for the adsorption species of CH_4 and CO_2 on Ru-CeO_2/MZ and are shown in figures 4 and 5. The obtained spectra referred to the spectra of the degassed catalysts at 450 °C prior to gas admission. As shown in figure 4, Ru-CeO_2/MZ displays bands at

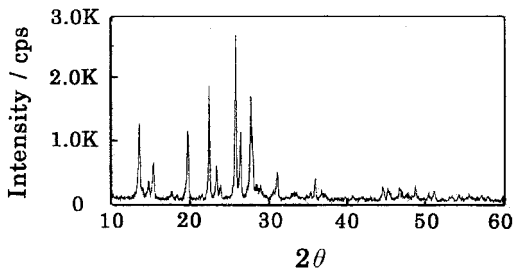

Figure 3. X-ray diffraction patterns of Ru-CeO_2/MZ.

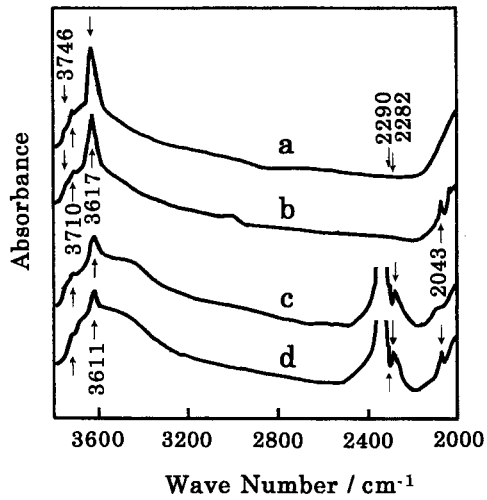

Figure 4. IR spectra in the range of 3800-2000 cm^{-1}. (a) Evacuation of Ru-CeO_2/MZ at 400 °C for 2 h. (b) Sample (a) exposed at 400 °C for 10 min to 0.1 kPa of CH_4. (c) Sample (a) exposed at 400 °C for 10 min to 0.1 kPa of CO_2. (d) Sample (a) exposed at 400 °C for 10 min to 0.2 kPa of the mixture gas of CH_4 and CO_2 (1 : 1).

3710, 3746, 3617 and 3611 cm^{-1} assigned to the located hydroxyl group [29]. The adsorption of CH_4 on Ru-CeO_2/MZ displays bands at 2043 cm^{-1} and around 2980 cm^{-1} (figure 4(b)). The adsorption of CO_2 on Ru-CeO_2/MZ displays bands at 2290, 2282, 1987, 1972 and 1375 cm^{-1}, and around 2080 cm^{-1} (figures 4(c) and 5(c)). The CO_2 adsorption shifts the band at 3617 cm^{-1}, due to the located hydroxyl group, to 3611 cm^{-1} and reduces its intensity. The CO_2 adsorption simultaneously gives a broad band around 3500 cm^{-1} assigned to a stretching vibration of O–H in hydrogen-bonded hydroxyl groups

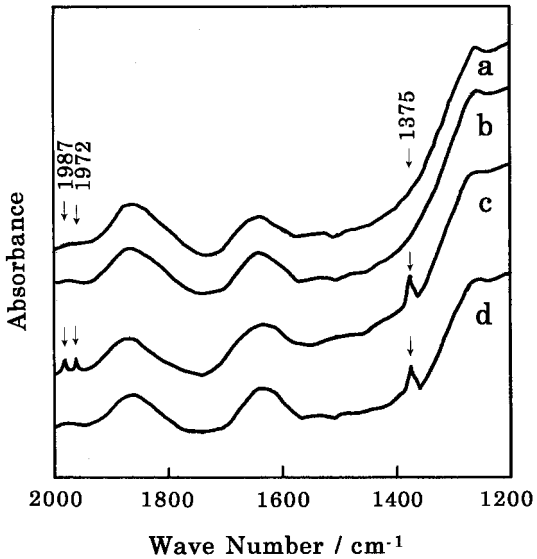

Figure 5. IR spectra in the range of 2000–1200 cm^{-1}. (a) Evacuation of Ru-CeO_2/MZ at 400 °C for 2 h. (b) Sample (a) exposed at 400 °C for 10 min to 0.1 kPa of CH_4. (c) Sample (a) exposed at 400 °C for 10 min to 0.1 kPa of CO_2. (d) Sample (a) exposed at 400 °C for 10 min to 0.2 kPa of the mixture gas of CH_4 and CO_2 (1 : 1).

(figure 4(c)). The adsorption of CH_4 and CO_2 on Ru-CeO_2/MZ displays bands at 2290, 2282, 2043, 2022 and 1375 cm^{-1}. A coordinated and adsorbed CO_2 displays bands, resulting from CO_2 ν_3 vibration, around the range 2200–2350 cm^{-1}. On the monometallic Ru/ZSM-5 samples, absorption of CO led to a band at 2046 cm^{-1}, due to CO stretching frequencies of CO linearly adsorbed on Ru^0 and several bands at higher frequencies related to CO on $Ru^{\delta+}$ species [30]. A ruthenium carbonium cluster displays 12 bands at 2078(m), 2058(vs), 2037(sh), 2032(vs), 2019(s), 2010(m), 2000(s), 1989(w), 1981(sh), 1963(w), 1950(w) and 1831(m) cm^{-1}, resulting from the stretching vibration of CO [31]. The adsorption of CO_2 on Ru-CeO_2/MZ displays bands at 2290, 2282, 1987, 1972 and 1374 cm^{-1} and around 2080 cm^{-1} (figures 4(c) and 5(c)). The bands at 2290 and 2282 cm^{-1} are attributed to CO_2 ν_3 vibration of CO_2 adsorbed on different sites. The bands at 2043, 2022 and around 2080 cm^{-1} are attributable to CO stretching frequencies of CO linearly adsorbed on Ru and/or to those of ruthenium carbonium. The appearance of the band at 2043 and 2022 cm^{-1} in the absence of CO_2 (figure 4(b)) is explainable in terms of the oxidation of some dissociative adsorption species of CH_4 with the storage oxygen of CeO_2 to CO or CO_2; ceria has an ability to store oxygen. The bands at 1987 and 1972 cm^{-1} are attributable to CO stretching frequencies of CO species like ruthenium carbonyl. The bands at 1987 and 1972 cm^{-1} disappear on adding CH_4 (figure 5(d)). The results strongly suggest that the carbonyl species must make some contribution to the reforming, and indicate that the addition of CH_4 remarkably moderates the surface concentration of Ru-CO species. In addition, the results indicate that a dissociative adsorption of CO_2 occurs in Ru-CeO_2/MZ, following the formation of ruthenium carbonyl. Furthermore, carbonate salts display bands, resulting from CO_3^{2-} ν_2 out-of-plane perpendicular vibration, in the region of 1450–1300 cm^{-1}; monodentate carbonate ions at ~1350 cm^{-1} [32], rare earth carbonate at ~1370 cm^{-1} [33], and formate at 1566 and 1375 cm^{-1} [2]. The assignment of the band at 1375 cm^{-1} to formate would essentially be excluded by limiting the formation of formate through the absence of hydrogen sources, since the adsorption of CO_2 also displays the band at 1375 cm^{-1} (figure 4(c)). The results indicate that some parts of CO_2 adsorb on ceria as carbonate ions. The red shift and decrease in the intensity of the band at 3617 cm^{-1} are likely explainable in terms of an interaction of adsorption species of CO_2 with located hydroxyl groups, such as hydrogen bonding. The adsorption species may cause the appearance of a hydrogen-bonded hydroxyl group. On adsorbing CH_4, a weak band around 2980 cm^{-1} appears (figure 4(b)). IR absorption, arising from the stretching vibration of C–H in CH_x, occurs in bands in the general range around 2840–3000 cm^{-1} [34]. The band around 2980 cm^{-1} is attributed to the stretching vibration of C–H in CH_x. The band around 2980 cm^{-1} disappears on adding CO_2 (figure 4(d)). The disappearance substantiates the conclusion that the decomposition of CH_4 is accelerated by CO_2.

The amount of hydrogen chemisorption was measured to study an average size of the fine particles of ruthenium. The amount is determined to be 2.1×10^{-5} mol g cat^{-1} at 25 °C at 1.0 kPa of H_2 pressure. No hydrogen chemisorbed on CeO_2/MZ under the same conditions. On the other hand, the amount of ruthenium loaded on the catalyst is calculated to be 2.9×10^{-5} mol g cat^{-1} from the chemical composition in table 1 and the atomic mass of ruthenium. On assuming that a hydrogen molecule chemisorbs on one surface atom of ruthenium, the number of chemisorption sites of H_2 at 25 °C at 1.0 kPa of H_2 pressure possess 72% of the amount of the supported ruthenium. The results indicate that the ruthenium is highly dispersed in the zeolite as fine particles. After the exposure of Ru-CeO_2/MZ at 450 °C for 24 h to 8 kPa of the reaction mixture gas of CO_2 and CH_4 in a proportion of $CO_2:CH_4 = 1:1$, the amount of hydrogen chemisorption decreased from 2.1 to 1.1×10^{-5} mol g cat^{-1} at 25 °C at 1.0 kPa of H_2 pressure. The decrease indicates the decrease in the surface area of ruthenium, that is, the aggregation of ruthenium particles occurs.

4. Conclusions

A catalyst consisting of ruthenium and CeO_2 highly dispersed on mordenite has been prepared. The reforming of CH_4 with CO_2 over Ru-CeO_2/MZ selectively forms H_2 and CO and the ratio of CO to H_2 is nearly equal to 1 in each experiment, whereas no reforming proceeds in the absence of Ru. The turnover frequency value is estimated to be 1.7 and 7.0 s^{-1} at 400 and 450 °C, respectively. The value is very high, compared with that of the other noble-metal catalysts. On the other hand, the decomposition rate of CH_4 is very slow, compared with the reforming rate. The results indicate that the presence of CO_2 significantly accelerates the CH_4 decomposition over Ru-CeO_2/MZ. The increase in catalytic weight due to a carbon formation reaction during the reforming is scarcely observed in Ru-CeO_2/MZ. The results hence indicate that carbon deposits resulting from CH_4 decomposition and CO_2 dissociation scarcely occur in the reforming. It is concluded that the presence of CO_2 accelerates the reforming process and depresses carbon formation. IR spectra for CO_2 adsorption give the bands at 1987 and 1972 cm^{-1} and around 2080 cm^{-1}, resulting from Ru-CO, and the band at 1375 cm^{-1} due to carbonate ion. The adsorption of CH_4 displays the bands at 2043 and 2022 cm^{-1} arising from Ru-CO and the band around 2980 cm^{-1} assigned to a stretching vibration of C–H in CH_x. Moreover, the adsorption of $CH_4 + CO_2$ displays bands at 2043 and 1375 cm^{-1}, but the bands at 2022, 1987 and

1972 cm^{-1} and around 2980 and 2080 cm^{-1} disappear. The results indicate that the reforming proceeds *via* the formation of the intermediate species such as Ru-CO, and Ru-CH_x on the surface of ruthenium. On assuming that a hydrogen molecule chemisorbs on one surface atom of ruthenium, the number of chemisorption sites of H_2 at 25 °C at 1.0 kPa of H_2 pressure possess 72% of the amount of the supported ruthenium. The results indicate that ruthenium is highly dispersed in the zeolite as fine particles. The data of H_2 adsorption support the idea that ruthenium is highly dispersed in the Ru-CeO_2/MZ.

References

[1] L. Basini and D. Sanfilippo, J. Catal. 157 (1995) 162.
[2] A.M. Efstathiou, A. Kladi, V.A. Tsipouriari and X.E. Verykios, J. Catal. 158 (1996) 64.
[3] M. Ito, T. Tagawa and S. Goto, Appl. Catal. A 177 (1999) 15.
[4] Z. Zhang, X.E. Verykios, S.M. MacDonald and S. Affrossman, J. Phys. Chem. 100 (1996) 744.
[5] K. Fujimoto, F.H. Ribeiro, M. Avalos-Borja and E. Iglesia, J. Catal. 179 (1998) 431.
[6] K. Tomishige, Y.-G. Chen and K. Fujimoto, J. Catal. 181 (1999) 91.
[7] S. Wang and G.Q. Lu. Appl. Catal. A 169 (1998) 271.
[8] J.H. Bitter, K. Seshan and J.A. Lercher, J. Catal. 183 (1999) 336.
[9] S. Ito, K. Nagashima, R. Araki, T. Yarimizu, S. Kameoka and K. Kunimori, Nippon Kagaku Kaishi (2000) 561.
[10] K. Nagaoka, K. Seshan, K. Aika and J.A. Lercher, J. Catal. 197 (2001) 34.
[11] E.C. Su and W.G. Rothschild, J. Catal. 99 (1986) 506.
[12] B. Harrison, A.F. Diwell and C. Hallett, Platinum Metals Rev. 32 (1988) 73.
[13] K.C. Taylor, Chemtech 20 (1990) 551.
[14] J.L. Duplan and H. Praliaud, Appl. Catal. 67 (1991) 325.
[15] J.C. Summers and S.A. Ausen, J. Catal. 58 (1979) 131.
[16] R.K. Kerz and J.A. Sell, J. Catal. 94 (1985) 166.
[17] B.K. Cho, J. Catal. 131 (1991) 74.
[18] P. Fornasiero, R.D. Monte, G.R. Rao, J. Kašpa, S. Mariani, A. Trovarelli and M. Graziani, J. Catal. 151 (1995) 168.
[19] K. Hashimoto, K. Matsuo, H. Kominami and Y. Kera, J. Chem. Soc. Faraday Trans. 93 (1997) 3729.
[20] K. Hashimoto and N. Toukai, J. Mol. Catal. 161 (2000) 174.
[21] M.F. Mark and W.F. Maier, J. Catal. 164 (1996) 122.
[22] M.C.J. Bradford and M.A. Vannice, J. Catal. 173 (1998) 157.
[23] J.H. Bitter, W. Hall, K. Seshan, J.G. van Ommen and J.A. Lercher, Catal. Today 29 (1996) 349.
[24] E.G.M. Kuijpers, J.W. Jansen, A.J. van Dillen and J.W. Geus, J. Catal. 72 (1981) 75.
[25] A. Erdőhelyi, J. Cserényi and F. Solymosi, J. Catal. 141 (1993) 287.
[26] *Powder Diffraction File: Inorganic*, Joint Committee on Powder Diffraction Standards, JCPDS, International Center for Diffraction Data, JCPDS 31-1268.
[27] *Powder Diffraction File: Inorganic*, Joint Committee on Powder Diffraction Standards, JCPDS, International Center for Diffraction Data, JCPDS 34-394.
[28] *Powder Diffraction File: Inorganic*, Joint Committee on Powder Diffraction Standards, JCPDS, International Center for Diffraction Data, JCPDS 6-663.
[29] J.B. Peri, J. Phys. Chem. 69 (1965) 220.
[30] C. Carmelo, S. Salvatore, M. Sinoma, M. Rosario and G. Signorino, Appl. Surf. Sci. 99 (1996) 401.
[31] K.K.H. Lee and W.T. Wong, Inorg. Chem. 35 (1996) 5393.
[32] J.W. London and A.T. Bell, J. Catal. 31 (1973) 32.
[33] Y. Wu, S. Motoi, K. Sugiyama, T. Matsuda and Y. Yoshida, Nippon Kagaku Kaishi (2000) 613.
[34] R.M. Silverstein and G.C. Bassler, *Spectrometric Identification of Organic Compounds* (Wiley, New York, 1963), p. 55.